

Damping control in viscoelastic beam dynamics

Elena Pierro¹

¹*Scuola di Ingegneria, Università degli Studi della Basilicata, 85100 Potenza, Italy*

Abstract

Viscoelasticity plays a key role in many practical applications and in different research fields, such as in seals, sliding-rolling contacts and crack propagation. In all these contexts, a proper knowledge of the viscoelastic modulus is very important. However, the experimental characterization of the frequency dependent modulus, carried out through different standard procedures, still presents some complexities, then possible alternative approaches are desirable. For example, the experimental investigation of viscoelastic beam dynamics would be challenging, especially for the intrinsic simplicity of this kind of test. This is why, a deep understanding of damping mechanisms in viscoelastic beams results to be a quite important task to better predict their dynamics. With the aim to enlighten damping properties in such structures, an analytical study of the transversal vibrations of a viscoelastic beam is presented in this paper. Some dimensionless parameters are defined, depending on the material properties and the beam geometry, which enable to shrewdly design the beam dynamics. In this way, by properly tuning such disclosed parameters, for example the dimensionless beam length or a chosen material, it is possible to enhance or suppress some resonant peaks, one at a time or more simultaneously. This is a remarkable possibility to efficiently control damping in these structures, and the results presented in this paper may help in elucidating experimental procedures for the characterization of viscoelastic materials.

I. INTRODUCTION

Nowadays, viscoelastic materials are widely utilized in several engineering applications, such as seals [1] and adhesives/biomimetic adhesives [2–5]. Moreover, they are object of recent research investigations, for example: (i) rolling contacts [6–8], (ii) sliding contacts [9–12], (iii) crack propagation [13–15], (iv) viscoelastic dewetting transition [16]. In all the aforementioned research fields, having knowledge of the correct viscoelastic modulus in the frequency domain is of utmost importance. Very often, viscoelastic materials are also combined with fibers or fillers, but also in this case, the mechanical behaviour of the viscoelastic matrix must be well established, especially as input data for numerical simulations. Usually, viscoelastic modulus is experimentally characterized, and one of the most utilized technique is the DMA (Dynamic mechanical analysis) [17], which is quite complex and time consuming. Alternative approaches have been presented in literature, such as the experimental dynamic evaluation of the viscoelastic beam-like structures [18–20]. Such experiments, however, require a good comprehension from a theoretical point of view of the viscoelastic beam dynamics. Many theoretical studies on the dynamics of non-viscous damped oscillators, for both SDOF [21, 22], and MDOF [23, 24] systems, have been presented in literature. Also viscoelastic continuous systems have been theoretically and experimentally investigated in their dynamics, such as beams and plates [25–27]. However, most of these studies do not present a qualitative analysis of the dynamic characteristics of such systems, in terms of eigenvalues and their connection with the most representative physical parameters. Only in Ref. [28], a deep analysis of a single degree-of-freedom non-viscously damped oscillator has been presented. Extending this kind of investigation to continuous systems would be of crucial concern when viscoelastic properties of materials must be properly established. With the aim to shed light on the vibrational behaviour of such systems, in this paper a detailed study of the dynamics of a viscoelastic beam is presented. Recall that the viscoelastic materials are characterized by the most general stress-strain relation [29]

$$\sigma(x, t) = \int_{-\infty}^t G(t - \tau) \dot{\varepsilon}(x, \tau) d\tau \quad (1)$$

where $\dot{\varepsilon}(t)$ is time derivative of the strain, $\sigma(t)$ is the stress, $G(t - \tau)$ is the time-dependent relaxation function, which is related, in the Laplace domain, to the viscoelastic modulus $E(s)$ through the relation $E(s) = sG(s)$. Usually, a discrete version of $E(s)$ is utilized to

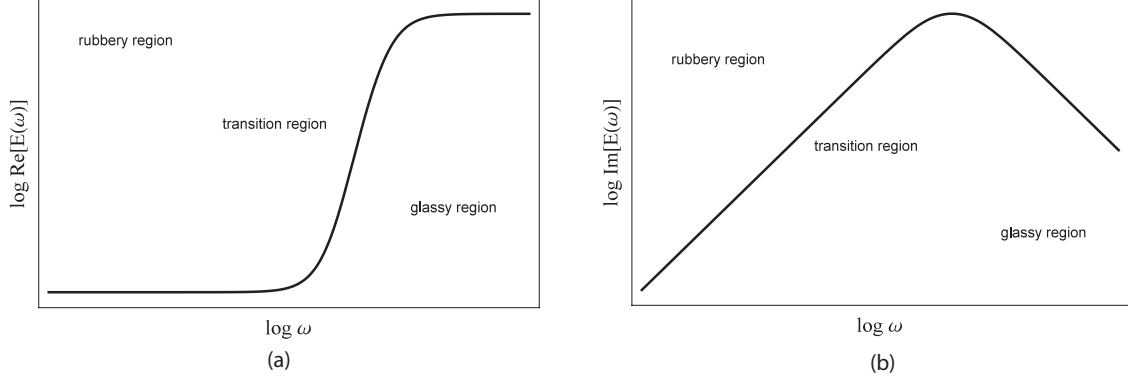


FIG. 1: The real part (a) and the imaginary part (b) of the elastic modulus $E(\omega)$ of a generic viscoelastic material.

characterize linear viscoelastic solids, which can be represented in the Laplace domain as

$$E(s) = E_0 + \sum_k E_k \frac{s\tau_k}{1 + s\tau_k} \quad (2)$$

where E_0 is the elastic modulus of the material at zero-frequency, τ_k and E_k are the relaxation time and the elastic modulus respectively of the generic spring-element in the generalized linear viscoelastic model [29]. The general trend of the viscoelastic modulus $E(\omega)$ is shown in Figure 1. It can be observed that at low frequencies the material is in the ‘rubbery’ region, indeed $\text{Re}[E(\omega)]$ is relatively small and approximately constant (Figure 1-a), and the viscoelastic dissipations related to the imaginary part $\text{Im}[E(\omega)]$ of the viscoelastic modulus becomes negligible (Figure 1-b). At very high frequencies the material is elastically very stiff (brittle-like). In this ‘glassy’ region $\text{Re}[E(\omega)]$ is again nearly constant but much larger (generally by 3 to 4 orders of magnitude) than in the rubbery region. The intermediate frequency range (the so called ‘transition’ region) determines the energy dissipation, and can completely deviate the modal behaviour of a viscoelastic solid from the equivalent elastic one. Moreover, the transition region, and hence the functions $\text{Re}[E(\omega)]$ and $\text{Im}[E(\omega)]$, can be shifted towards higher or smaller frequencies by simply varying temperature, because of the viscoelastic modulus $E(\omega)$ dependence on temperature [29]. Of course, only the knowledge of the analytical vibrational response of a viscoelastic structure can provide the right parametric quantities, useful to accurately enlighten the relationship between the material properties and the modal contents. In this direction, the flexural vibrations of a viscoelastic beam is analytically studied in this paper, and by introducing some non-dimensional pa-

rameters, a qualitative analysis of the eigenvalues is presented. At first, an ideal viscoelastic material is considered, i.e. characterized by one single relaxation time. This kind of study, indeed, is useful for a first understanding of the physical parameters enclosed in the problem. Then, two relaxation times are taken into account, and their influence on the dynamics of the beam is deeply evaluated and described. Finally, some considerations are pointed out regarding the vibrational response of the beam in case of real viscoelastic materials.

II. THE MODEL

In this section the analytical dynamic response of a viscoelastic beam with rectangular cross section is derived. Let be L , W , and H respectively the length, the width and the thickness of the beam (Figure 2), and let us assume that $L \gg W$, $L \gg H$. Assuming also that the displacement along the z -axis $|u(x, t)| \ll L$, the Bernoulli theory of transversal vibrations can be applied and therefore it is possible to neglect the influence of shear stress in the beam. It is worth noticing that this hypothesis does not limit the validity of the analysis, since the attention is paid to the first resonant peaks, which are not affected by shear deformations. Hence, the general equation of motion is [30]

$$J_{xz} \int_{-\infty}^t E(t - \tau) \frac{\partial^4 u(x, \tau)}{\partial x^4} d\tau + \mu \frac{\partial^2 u(x, t)}{\partial t^2} = f(x, t) \quad (3)$$

where $\mu = \rho A$, ρ is the bulk density of the material the cantilever is made of, A is the area of the cross section of the beam, i.e. $A = WH$, $J_{xz} = (1/12)WH^3$, and $f(x, t)$ is the generic forcing term. It must be highlighted that some additional terms could be considered in Eq.(3), representing different kind of damping contributes [31] (e.g. viscous damping and hysteresis damping). In the present study such terms are neglected, but it is important to underline that the results obtained in this paper are not affected by this assumption from a qualitative point of view. The forced solution of the above problem Eq.(3) can be found in the form of a series of the eigenfunction $\phi_n(x)$ of the following problem

$$J_{xz} \int_{-\infty}^t E(t - \tau) u_{xxxx}(x, \tau) d\tau + \mu u_{tt}(x, t) = 0 \quad (4)$$

$(u_x(x, t) = \partial u(x, t) / \partial x, u_t(x, t) = \partial u(x, t) / \partial t)$, with the opportune boundary conditions. In this study, the free-free boundary conditions are considered

$$\begin{aligned} u_{xx}(0, t) &= 0 \\ u_{xxx}(0, t) &= 0 \\ u_{xx}(L, t) &= 0 \\ u_{xxx}(L, t) &= 0 \end{aligned} \tag{5}$$

. By Laplace transforming the time-dependence in Eq.(4), and considering equal to zero the initial conditions, it is easy to show that the eigenfunctions $\phi(x, s)$ must satisfy the following equation

$$\phi_{xxxx}(x) - \beta_{eq}^4(s) \phi(x) = 0 \tag{6}$$

where it is defined

$$\beta_{eq}^4(s) = -\frac{\mu s^2}{J_{xz}E(s)} = -\frac{\mu s^2}{J_{xz}}C(s) \tag{7}$$

and the compliance of the viscoelastic material $C(s) = 1/E(s)$. The boundary conditions then become

$$\begin{aligned} \phi_{xx}(0) &= 0 \\ \phi_{xxx}(0) &= 0 \\ \phi_{xx}(L) &= 0 \\ \phi_{xxx}(L) &= 0 \end{aligned} \tag{8}$$

The solution of the above Eq.(6) can be written in the form

$$\phi(x, s) = W_1 \cos[\beta_{eq}(s)x] + W_2 \sin[\beta_{eq}(s)x] + W_3 \cosh[\beta_{eq}(s)x] + W_4 \sinh[\beta_{eq}(s)x] \tag{9}$$

and by requiring that the determinant of the system matrix obtained from Eqs.(8) is zero, one obtains

$$[1 - \cos(\beta_{eq}L) \cosh(\beta_{eq}L)] = 0 \tag{10}$$

The solutions $\beta_n L = c_n$ of the above Eq.(10) are well known [30], and they are the same of the perfectly elastic case. In particular, from the following relation

$$-\frac{\mu s^2}{J_{xz}E(s)} = (\beta_n)^4 = \left(\frac{c_n}{L}\right)^4 \tag{11}$$

it is possible to calculate the complex conjugate eigenvalues s_n corresponding to the n_{th} mode, and the real poles s_k related to the material viscoelasticity (a detailed analysis of the eigenvalues will be shown in the next section). The values β_n allow to determine the eigenfunctions $\phi_n(x)$

$$\phi_n(x) = \cosh(\beta_n x) + \cos(\beta_n x) - \frac{\cosh(\beta_n L) - \cos(\beta_n L)}{\sinh(\beta_n L) - \sin(\beta_n L)} [\sinh(\beta_n x) + \sin(\beta_n x)] \quad (12)$$

which are equal to the eigenfunctions of the elastic case. A simple proof of the previous statement can be shown by considering the initial conditions $u(x, 0) = \phi_n(x)$ and $u_t(x, 0) = 0$ of the problem Eq.(4). In this case, indeed, the solution of Eq.(4) is $u(x, t) = C e^{\text{Re}[s_n]t} \phi_n(x) \cos(\text{Im}[s_n]t)$.

III. BEAM RESPONSE

In this section the solution of Eq.(3) is calculated, by considering (see Ref.[26]) the decomposition of the system response into the modes $\phi_n(x)$ of the beam

$$u(x, t) = \sum_{n=1}^{+\infty} \phi_n(x) q_n(t) \quad (13)$$

For the orthogonality condition one has

$$\frac{1}{L} \int_0^L \phi_n(x) \phi_m(x) dx = \delta_{nm} \quad (14)$$

where δ_{nm} is Kronecker delta function. Moreover, because of Eqs.(6)-(7), the following relation holds true

$$\frac{1}{L} \int_0^L (\phi_n)_{xxxx}(x) \phi_m(x) dx = \frac{1}{L} \int_0^L \phi_n(x) \beta_n^4 \phi_m(x) dx = \delta_{nm} \beta_n^4 \quad (15)$$

Let us project the equation of motion on the function $\phi_m(x)$ of the basis. The projected solution $u_m(t)$ is defined as

$$u_m(t) = \langle u(x, t) \phi_m(x) \rangle = \frac{1}{L} \int_0^L u(x, t) \phi_m(x) dx \quad (16)$$

therefore Eq.(3) becomes

$$\mu \ddot{q}_n(t) + J_{xz} \beta_n^4 \int_{-\infty}^t E(t - \tau) q_n(\tau) d\tau = f_n(t) \quad (17)$$

where $f_n(t) = \frac{1}{L} \int_0^L f(x, t) \phi_n(x) dx$ is the projected force term. By taking the Laplace Transform of Eq.(17), with initial conditions equal to zero, one obtains

$$\mu s^2 Q_n(s) + J_{xz} \beta_n^4 E(s) Q_n(s) = F_n(s) \quad (18)$$

It is possible to rewrite the above equation as

$$Q_n(s) = H_n(s) F_n(s) \quad (19)$$

where the function

$$H_n(s) = \frac{1}{[\mu s^2 + J_{xz} \beta_n^4 E(s)]} \quad (20)$$

is the Transfer Function of the system, for the n_{th} mode.

Eq.(13) can be therefore written in the Laplace domain as

$$U(x, s) = \sum_{n=1}^{+\infty} \phi_n(x) \frac{F_n(x, s)}{\mu s^2 + J_{xz} \beta_n^4 E(s)} \quad (21)$$

In particular, by considering as external applied force, a Dirac Delta of constant amplitude F_0 , in both the time and the spatial domains, the force can be written as $f(x, t) = F_0 \delta(x - x_f) \delta(t - t_0)$. Therefore in the Laplace domain it becomes

$$F_n = \int_0^L F_0 \delta(x - x_f) \phi_n(x) dx = F_0 \phi_n(x_f) \quad (22)$$

and finally the system response is

$$U(x, s) = F_0 \sum_{n=1}^{+\infty} \frac{\phi_n(x) \phi_n(x_f)}{\mu s^2 + J_{xz} \beta_n^4 E(s)} \quad (23)$$

IV. VISCOELASTIC MODEL - SYSTEM EIGENVALUES

Let us first consider an ideal viscoelastic material with a single relaxation time τ_1 , whose elastic properties can be represented by the modulus

$$E(s) = E_0 + E_1 \frac{\tau_1 s}{1 + \tau_1 s} \quad (24)$$

By substituting the previous complex function in Eq.(11), the characteristic equation for each n_{th} mode can be obtained

$$\tau_1 s^3 + s^2 + (E_0 + E_1) \tau_1 r_n s + r_n E_0 = 0 \quad (25)$$

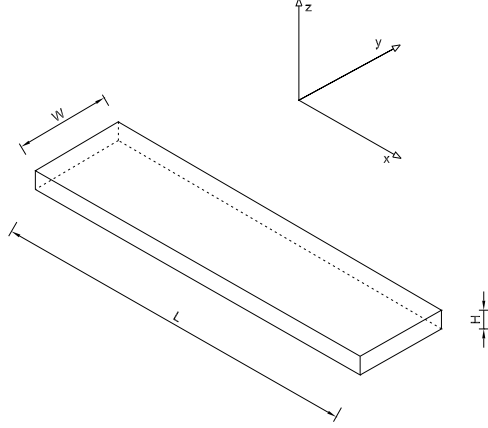


FIG. 2: Viscoelastic beam of length L , cross section area $A = WH$.

where $r_n = (\beta_n)^4 J_{xz}/\mu$. Notice that the solutions of the cubic equation Eq.(25) can be i) one real root and two complex conjugate roots, ii) all roots real. This means that one eigenvalue is always related to an overdamped motion. When the other two eigenvalues are complex conjugate, they represent the oscillatory contribute of the n_{th} mode in the beam dynamics. Otherwise, in case of three real roots, the n_{th} mode is not oscillatory.

With regards to the transverse motions of a narrow, homogenous beam with a bending stiffness $E_0 J_{xz}$ and density ρ , the value of the natural frequencies can be calculated using a simple formula which is always valid, regardless of the boundary conditions [32]:

$$\omega_n = \left(\frac{c_n}{L}\right)^2 \sqrt{\frac{E_0 J_{xz}}{\rho A}} \quad (26)$$

where coefficient c_n depends on the specific boundary conditions. The first natural frequency, in particular, can be written as

$$\omega_1 = \alpha^2 \delta_1 \quad (27)$$

being $\delta_1 = c_1^2 \sqrt{E_0 A / (\rho J_{xz})}$, and $\alpha = R_g / L$ the dimensionless beam length, with $R_g = \sqrt{J_{xz} / A}$ the radius of gyration. For the rectangular beam cross section under investigation (Figure 2), one has $\alpha = H / (\sqrt{12}L)$ and $\delta_1 = (c_1^2 / H) \sqrt{12 E_0 / \rho}$. The non-dimensional eigenvalue is now defined

$$\bar{s} = s / \delta_1 \quad (28)$$

and in particular one has, for the n_{th} mode, $\omega_n^2 = E_0 \beta_n^4 J_{xz} / \mu = r_n E_0$ and $\delta_n = c_n^2 \sqrt{E_0 A / (\rho J_{xz})}$.

By substituting Eq.(28) in Eq.(25), the following non-dimensional characteristic equation is obtained

$$\bar{s}^3 + \bar{s}^2 \frac{1}{\theta_1} + (1 + \gamma_1) \alpha^4 \Delta_n^2 \bar{s} + \frac{1}{\theta_1} \alpha^4 \Delta_n^2 = 0 \quad (29)$$

where $\Delta_n = \delta_n / \delta_1$, and having defined the dimensional groups

$$\theta_1 = \delta_1 \tau_1 \quad (30)$$

$$\gamma_1 = E_1 / E_0 \quad (31)$$

. Eq.(29) can be then re-written as

$$\bar{s}^3 + \sum_{j=0}^2 a_j^j \bar{s}^j = 0 \quad (32)$$

where $a_0 = (1/\theta_1) \alpha^4 \Delta_n^2$, $a_1 = (1 + \gamma_1) \alpha^4 \Delta_n^2$, $a_2 = 1/\theta_1$.

By defining

$$Q = \frac{3a_1 - a_2^2}{9} \quad (33)$$

$$R = \frac{9a_2a_1 - 27a_0 - 2a_2^3}{54} \quad (34)$$

the discriminant of Eq.(32) is $D = Q^3 + R^2$, and the solutions of Eq.(32) can be therefore written as [33]

$$\begin{aligned} \bar{s}_1 &= -\frac{a_2}{3} - \frac{1}{2}(S + T) + i\frac{\sqrt{3}}{2}(S - T) \\ \bar{s}_2 &= -\frac{a_2}{3} - \frac{1}{2}(S + T) - i\frac{\sqrt{3}}{2}(S - T) \\ \bar{s}_3 &= -\frac{a_2}{3} + (S + T) \end{aligned} \quad (35)$$

where $S = \sqrt[3]{R + \sqrt{D}}$ and $T = \sqrt[3]{R - \sqrt{D}}$. In our case, the discriminant D , indicated as $D_1(n)$, is function of n , i.e. of the number of the n_{th} mode considered

$$D_1(n) = \frac{\alpha^4 \Delta_n^2 \{4 + \alpha^4 \Delta_n^2 \theta_1^2 [8 - \gamma_1 (20 + \gamma_1) + 4\alpha^2 (1 + \gamma_1)^3 \Delta_n^2 \theta_1^2]\}}{108\theta_1^4} \quad (36)$$

This function $D_1(n)$ plays a key role in the understanding the nature of the roots of Eq.(32), as it will be widely discussed in Section III.

At last, the beam cross-section acceleration $A(x, s)$ in terms of the above defined non-dimensional groups is formulated, considering that $A(x, s) = s^2 U(x, s)$ (see Eq.(23))

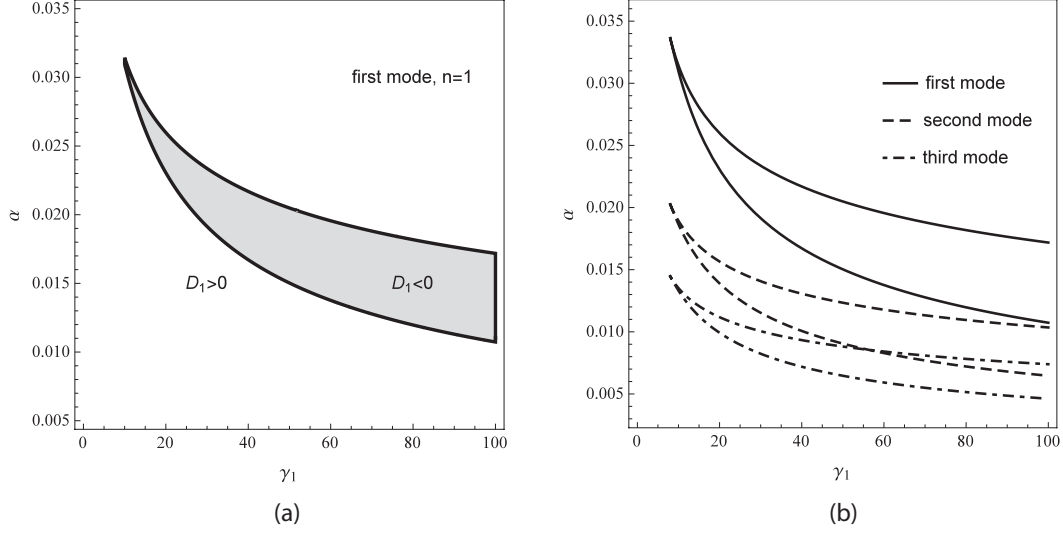


FIG. 3: The region map for the first flexural mode of the beam $n = 1$, for $\theta_1 = \bar{\theta}_1$ (a). The shaded area indicates the parameter (α, γ_1) combinations which determine the suppression of the first peak. Similar region maps are shown, for the first three modes $n = 1, 2, 3$ (b). Interestingly, for several values of α and γ_1 , some areas at $D_1(n) < 0$ are overlapped, determining the suppression of more peaks simultaneously.

$$A(x, \bar{s}) = F_0 \sum_{n=1}^{+\infty} \frac{\bar{s}^2 (1 + \theta_1 \bar{s}) \phi_n(x) \phi_n(x_f)}{\mu \theta_1 (\bar{s}^3 + \sum_{j=0}^2 a_j \bar{s}^j)} \quad (37)$$

being $\phi_n(x)$ the eigenfunctions defined in Eq.(12).

More realistically, a second relaxation time contribute is now included in the viscoelastic modulus $E(s)$, which therefore becomes

$$E(s) = E_0 + E_1 \frac{\tau_1 s}{1 + \tau_1 s} + E_2 \frac{\tau_2 s}{1 + \tau_2 s} \quad (38)$$

Following the same approach previously described, the fourth-order characteristic equation for each n_{th} mode can be obtained

$$\bar{s}^4 + \sum_{j=0}^3 a_j \bar{s}^j = 0 \quad (39)$$

where

$$\begin{aligned}
a_0 &= \alpha^4 \Delta_n^2 \frac{1}{\theta_1 \theta_2} \\
a_1 &= \left(\frac{1}{\theta_2} + \frac{1}{\theta_1} + \frac{1}{\theta_2} \gamma_1 + \frac{1}{\theta_1} \gamma_2 \right) \alpha^4 \Delta_n^2 \\
a_2 &= \left(\frac{1}{\theta_1 \theta_2} + \alpha^4 \Delta_n^2 + \alpha^4 \Delta_n^2 \gamma_1 + \alpha^4 \Delta_n^2 \gamma_2 \right) \\
a_3 &= \left(\frac{1}{\theta_1} + \frac{1}{\theta_2} \right)
\end{aligned} \tag{40}$$

having defined $\gamma_2 = E_2/E_0$ and $\theta_2 = \tau_2 \delta_1$. Moreover, it is possible to define, for the quartic equation Eq.(39), the discriminant $D_2(n)$ [34]-[35]

$$\begin{aligned}
D_2(n) &= 256a_0^3 - 192a_3a_1a_0^2 - 128a_2^2a_0^2 + 144a_2a_1^2a_0 - 27a_1^4 + 144a_3^2a_2a_0^2 - 6a_3^2a_1^2a_0 - 80a_3a_2^2a_1a_0 + \\
&\quad + 18a_3a_2a_1^3 + 16a_2^4a_0 - 4a_2^3a_1^2 - 27a_3^4a_0^2 + 18a_3^3a_2a_1a_0 - 4a_3^3a_1^3 - 4a_3^2a_2^3a_0 + a_3^2a_2^2a_1^2
\end{aligned} \tag{41}$$

which can be utilized to deduce important properties of the roots of Eq.(39).

The beam cross-section acceleration $A(x, \bar{s})$ is in this case

$$A(x, \bar{s}) = F_0 \sum_{n=1}^{+\infty} \frac{\bar{s}^2 (1 + \theta_1 \bar{s}) (1 + \theta_2 \bar{s}) \phi_n(x) \phi_n(x_f)}{\mu \theta_1 \theta_2 \left(\bar{s}^4 + \sum_{j=0}^3 a_j \bar{s}^j \right)} \tag{42}$$

V. RESULTS

In this section the main results of the presented analysis are discussed. The flexural vibrations of a viscoelastic beam with rectangular cross section and thickness $H = 1$ [cm], which oscillates in the xz -plane (Figure 2) are studied. The only geometrical parameter which is considered varying in calculations, is the beam length L . In particular, the ratio $\alpha = R_g/L$ is changed maintaining $R_g = H/\sqrt{12}$ constant. The main scope of the paper is not a quantitative investigation of a specific viscoelastic material, but a qualitative study of a generic viscoelastic beam behaviour, which can be considered at different lengths L (e.g. in experimental testing campaigns, to cover wide frequency ranges) and at different working temperatures (i.e. with varying elastic coefficients E_k and relaxation times τ_k). In this view, the two material properties considered constant in the numerical calculations are

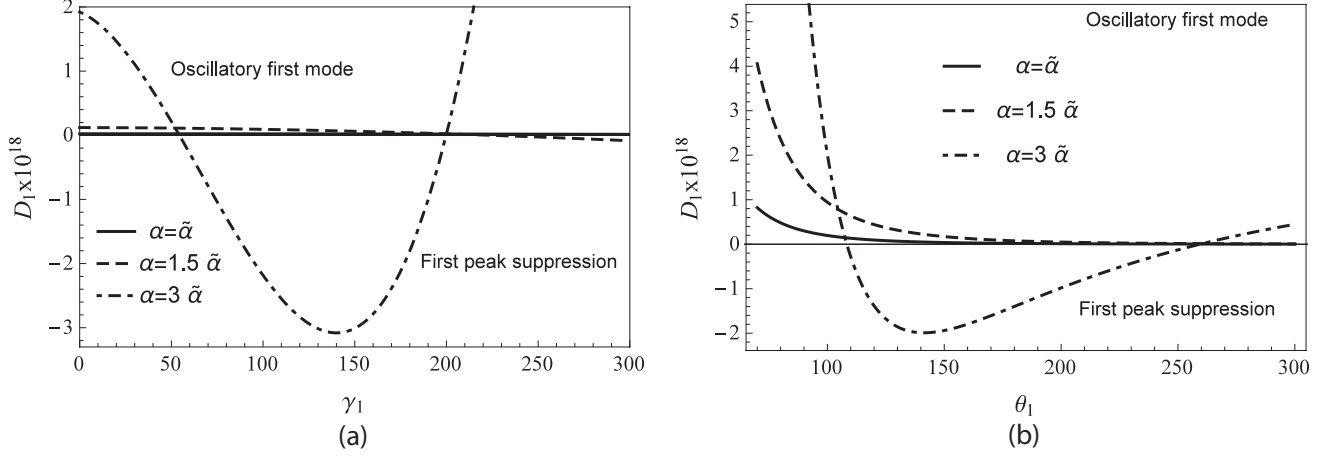


FIG. 4: The discriminant $D_1(1)$ for the first mode $n = 1$, as a function of γ_1 , for $\theta_1 = \bar{\theta}_1$ (a), and as a function of θ_1 , for $\gamma_1 = \bar{\gamma}_1$ (b), for different values of α , i.e $\alpha = \tilde{\alpha}$ (solid line), $\alpha = 1.5 \tilde{\alpha}$ (dashed line), $\alpha = 3 \tilde{\alpha}$ (dot-dashed line).

$\rho = 1180 \text{ [kg m}^{-3}\text{]}$ and $E_0 = 2.24 * 10^6 \text{ [Pa]}$ of a typical viscoelastic material, i.e. PMMA (polymethyl methacrylate) [36]. Therefore the parameters δ_n are constant and, in particular, $\delta_1 = 3.4 * 10^5$ for the first flexural mode of the beam. The other properties E_1 , E_2 , τ_1 and τ_2 are taken varying in the analysis, however $\bar{\gamma}_1 = E_1/E_0 = 87$ and $\bar{\gamma}_2 = E_2/E_0 = 126$ of PMMA are considered as reference. Moreover, the relaxation times for the frequency range under study give the reference values $\bar{\theta}_1 = \delta_1 \tau_1 = 170$, $\bar{\theta}_2 = \delta_1 \tau_2 = 6700$. The numerical values here considered, are simply representative of a real viscoelastic material but, thanks to the dimensional analysis presented in the paper, can be substituted with the constants of any other viscoelastic material, thus not modifying the qualitative results.

At first, let us consider an ideal viscoelastic material with one relaxation time τ_1 , and elastic coefficients E_0 and E_1 (Eq.24). For each n_{th} mode, the three eigenvalues (see Eq.(35)) can be calculated. The two complex conjugate eigenvalues represent the oscillatory counterpart of the beam n_{th} mode. The real eigenvalue gives rise to a pure dissipative contribute. However, when the discriminant $D_1(n)$, defined in Eq.(36), is negative $D_1(n) < 0$, all roots of Eq.(29) are real, and the n_{th} mode is not oscillatory. In Figure 3-a, a region map is shown, for the first flexural mode of the beam ($n = 1$), with $\theta_1 = \bar{\theta}_1$. The shaded area is obtained with the parameter values (α, γ_1) which give the condition $D_1(1) < 0$. Analogous maps, for the first three flexural modes of the beam, are represented by the correspondent

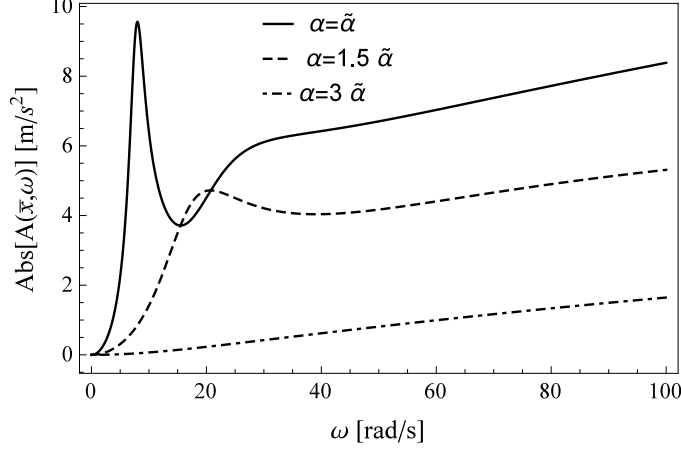


FIG. 5: The acceleration modulus $|A(\bar{x}, \omega)|$ of the viscoelastic beam with one relaxation time, in the section $x = x_f = \bar{x} = 0.4L$, for $\theta_1 = \bar{\theta}_1$, $\gamma_1 = \bar{\gamma}_1$, and for three different values of α , i.e. $\alpha = \tilde{\alpha}$ (solid line), $\alpha = 1.5\tilde{\alpha}$ (dashed line), $\alpha = 3\tilde{\alpha}$ (dot-dashed line). For $\alpha = 3\tilde{\alpha}$, being $D_1(1) < 0$, the first peak is suppressed.

curves in Figure 3-b, which are obtained by finding the two real solutions $\alpha = \alpha(\gamma_1)$ of the equation $D_1(n) = 0$, for $n = 1, 2, 3$. By properly combining the parameters (α, γ_1) , different peaks can be suppressed simultaneously, since the areas which give the condition $D_1(n) < 0$ for different values of n are overlapped. In particular, this means that, once the material is prescribed, i.e. for given values of θ_1 and γ_1 , the dynamics of the beam can be decisively modified by varying its length L . The sign of the discriminant $D_1(1)$, for the first mode, can be directly deduced by means of the curves plotted in Figure 4, where $D_1(1)$ is shown as a function of γ_1 (Figure 4-a), for $\theta_1 = \bar{\theta}_1$, and as a function of θ_1 , for $\gamma_1 = \bar{\gamma}_1$ (Figure 4-b), for different values of α , i.e. $\alpha = \tilde{\alpha}$ (solid line), $\alpha = 1.5\tilde{\alpha}$ (dashed line), $\alpha = 3\tilde{\alpha}$ (dot-dashed line), where it has been considered the reference beam length equal to $\tilde{L} = 60[\text{cm}]$, and therefore $\tilde{\alpha} = R_g/\tilde{L} = 0.0048$. In Figure 5 the system response is represented, in terms of the acceleration modulus $|A(\bar{x}, \omega)|$ (see Eq.37), evaluated at the beam section $x = x_f = \bar{x} = 0.4L$, for $\theta_1 = \bar{\theta}_1$ and $\gamma_1 = \bar{\gamma}_1$. Three different values of beam length L are considered, i.e. $\alpha = \tilde{\alpha}$ (solid line), $\alpha = 1.5\tilde{\alpha}$ (dashed line), $\alpha = 3\tilde{\alpha}$ (dot-dashed line), which give a clear first peak for $\alpha = \tilde{\alpha}$ and $\alpha = 1.5\tilde{\alpha}$, a suppressed first peak for $\alpha = 3\tilde{\alpha}$, being $D_1(1) < 0$ in the last case, as one can notice in Figure 4.

Let us consider now a viscoelastic material with two relaxation times, in order to explore

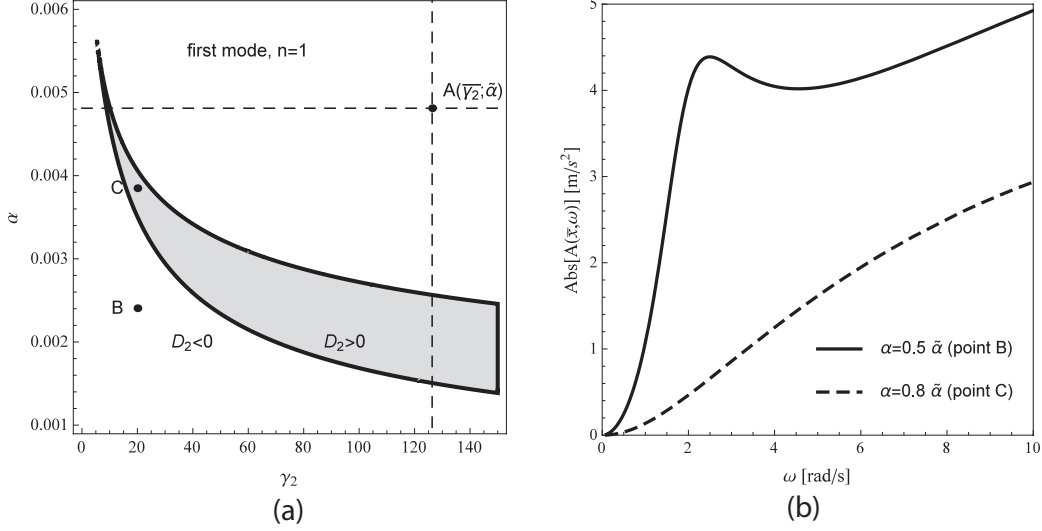


FIG. 6: The region map for the first flexural mode of the beam $n = 1$, with two relaxation times, for $\theta_1 = \bar{\theta}_1$, $\theta_2 = \bar{\theta}_2$, $\gamma_1 = \bar{\gamma}_1$: the shaded area indicates the parameter (γ_2, α) combinations which determine the suppression of the first peak (a). The acceleration modulus $|A(\bar{x}, \omega)|$ of the viscoelastic beam with two relaxation times is plotted, in the beam section $x = x_f = \bar{x} = 0.4L$, related to points $B(20; 0.5\bar{\alpha})$ and $C(20; 0.8\bar{\alpha})$.

possible variations in the beam dynamics. In Figure 6-a a region map is shown, for the first flexural mode of the beam ($n = 1$), with $\theta_1 = \bar{\theta}_1$, $\theta_2 = \bar{\theta}_2$, $\gamma_1 = \bar{\gamma}_1$. The shaded area is obtained with the parameter values (γ_2, α) compounds which give the condition $D_2(1) > 0$. Indeed, since the nature of the eigenvalues characteristic equation is changed, i.e. being Eq.(39) a quartic equation, the condition for an oscillatory mode is $D_2(n) < 0$ [34]-[35]. Point A in Figure 6-a is obtained by considering the reference parameters $(\bar{\gamma}_2, \bar{\alpha})$. Since it is far from the shaded area at $D_2(1) > 0$, it is related to a oscillatory first mode for small α variations. In order to better evaluate the influence of the parameter α , points B and C have been considered to calculate the frequency response of the beam. In Figure 6-b, the acceleration modulus $|A(\bar{x}, \omega)|$ (see Eq.42), calculated at the beam section $x = x_f = \bar{x} = 0.4L$, is shown for $\theta_1 = \bar{\theta}_1$, $\theta_2 = \bar{\theta}_2$, $\gamma_1 = \bar{\gamma}_1$, $\gamma_2 = 20$ and for $\alpha = 0.5\bar{\alpha}$ (solid line, point B of Figure 6-a), $\alpha = 0.8\bar{\alpha}$ (dashed line, point C of Figure 6-a). It is possible to observe that the curve obtained with $\alpha = 0.8\bar{\alpha}$ does not present the first peak, because of the considered parameters, which give in this case $D_2(1) > 0$.

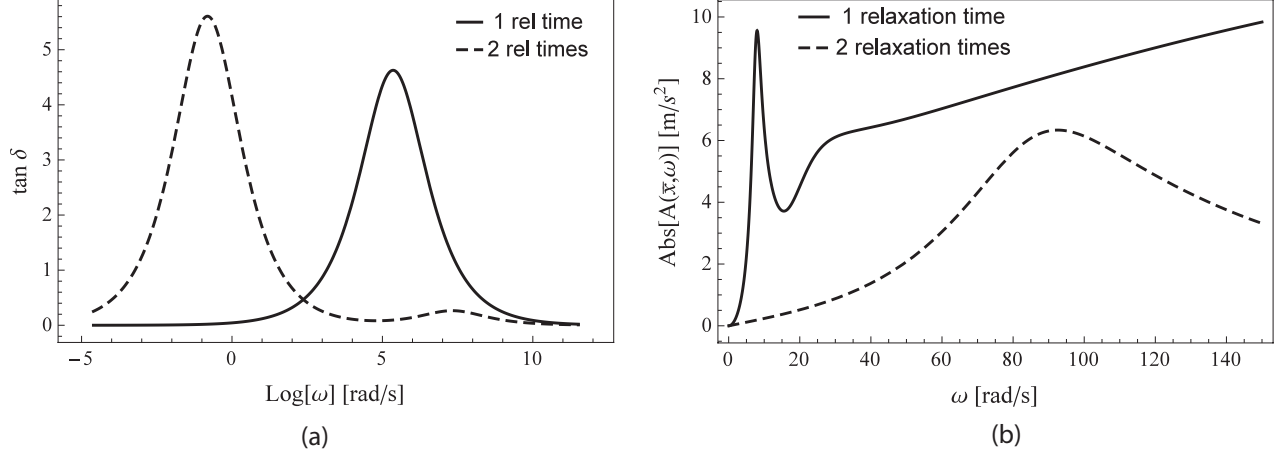


FIG. 7: The viscoelastic modulus $E(\omega)$, for one relaxation time, with $\theta_1 = \bar{\theta}_1$, $\gamma_1 = \bar{\gamma}_1$ (solid curve), and for two relaxation times, with $\theta_1 = \bar{\theta}_1$, $\gamma_1 = \bar{\gamma}_1$, $\theta_2 = \bar{\theta}_2$, $\gamma_2 = \bar{\gamma}_2$ (dashed curve), represented by the function $\tan \delta = \text{Re}[E(\omega)]/\text{Im}[E(\omega)]$ (a); the acceleration modulus $|A(\bar{x}, \omega)|$ is shown in the two cases, for $\alpha = \tilde{\alpha}$, $x = x_f = \bar{x} = 0.4L$, for one relaxation time (solid curve) and for two relaxation times (dashed curve) (b).

VI. FREQUENCY RESPONSES

Let us observe that, besides the sign of the discriminants $D_1(n)$ and $D_2(n)$, and the different values of α , which establish the possible n_{th} peak suppression, there is no significant difference in considering one or two relaxation times. In this respect, the spectrum of the viscoelastic modulus $E(\omega)$ is considered in the two cases, as shown in Figure 7-a, where the function $\tan \delta = \text{Re}[E(\omega)]/\text{Im}[E(\omega)]$ is plotted, for one relaxation time ($\theta_1 = \bar{\theta}_1$, $\gamma_1 = \bar{\gamma}_1$, solid curve), and for two relaxation times ($\theta_1 = \bar{\theta}_1$, $\gamma_1 = \bar{\gamma}_1$, $\theta_2 = \bar{\theta}_2$, $\gamma_2 = \bar{\gamma}_2$, dashed curve). It is evident that in the two cases, the transition region, where the function $\tan \delta$ reaches the maximum, thus determining the prominent energy dissipation, is differently positioned in the frequency spectrum. The correspondent acceleration moduli $|A(\bar{x}, \omega)|$ are shown in Figure 7-b, for $\alpha = \tilde{\alpha}$, $x = x_f = \bar{x} = 0.4L$, for one relaxation time (solid curve) and for two relaxation times (dashed curve). Notice that, in the case of two relaxation times the function $\tan \delta$ presents higher values, with respect to the one relaxation time case, in the range of frequencies where the first peak lies ($0 - 100 \text{ [rad s}^{-1}\text{]}$). This is why the first peak, when two relaxation times are considered, is more damped. It is important to

underline that, because of the intrinsic characteristics of viscoelastic materials [29], which see the viscoelastic modulus $E(\omega)$ depending on temperature, the above mentioned damping effect can be observed just modifying the surrounding temperature. Indeed, increasing or decreasing the working temperature, the functions $\text{Re}[E(\omega)]$ and $\text{Im}[E(\omega)]$ are shifted towards higher or smaller frequencies respectively (as well as and the function $\tan \delta$), and consequently the material damping is differently spread in frequency.

However, once the material is prescribed, i.e. the viscoelastic modulus $E(\omega)$ is defined with the related parameters, θ_1 and γ_1 for one relaxation time, $\theta_1, \theta_2, \gamma_1$ and γ_2 for two relaxation times, the dimensionless beam length α plays a crucial role in the possible overlapping of the first natural frequency ω_1 with the transition region. Moreover, in the hypothesis of linearity, such considerations can be extended to all the peaks, since the system can be decoupled and each vibration mode can be studied independently.

In conclusion, through the defined dimensionless parameters, it is possible to completely disclose the transversal vibrations of a viscoelastic beam. Suppressing certain peaks, by varying the beam length with α , or by changing the material properties (i.e. θ_1 and γ_1 for one relaxation time, $\theta_1, \theta_2, \gamma_1$ and γ_2 for two relaxation times) for example by modifying the surrounding temperature, is an appealing chance for different applications. In particular, it is important to stress that, although the real viscoelastic materials present more than two relaxation times, the number of relaxation times to be considered in modelling the beam dynamics, does not represent a limit of our study. Firstly, because it has been shown that there is not a considerable difference, from a qualitative point of view, by increasing the number of time relaxations. Furthermore, it is always possible to divide the frequency spectrum under analysis in several intervals, thus allowing the decreasing of the predominant time relaxations number in such intervals. Moreover, by varying the beam length, it is possible to study a wide frequency range, by focusing the attention only to the first resonant peaks, so that the (Euler-Bernoulli) hypothesis still remains valid.

Finally, it must be pointed out that this study can be utilized to properly interpret the viscoelastic beam vibrational spectrum, when a material characterization is carried out. This is an awkward task, indeed, since when a viscoelastic beam with an unknown material is experimentally studied, the resonant peaks positions are not so straightforward to be identified, as in the elastic case. This kind of experimental investigation is currently object of study, with the aim to characterize viscoelastic materials by means of the transversal

vibrations of beams with different lengths.

VII. CONCLUSIONS

In this paper an analytical study of the transversal vibrations of a viscoelastic beam has been presented. The analytical solution has been obtained by means of modal superposition. In particular, while the beam eigenfunctions are the same of the perfectly elastic case, the eigenvalues strongly depend on the material viscoelasticity, and they increase in number with the relaxation times of the viscoelastic modulus. In order to put in evidence the main characteristics of the beam dynamics, two cases have been considered, i.e. a viscoelastic material both with one single relaxation time and with two relaxation times. A dimensional analysis has been performed, which has disclosed the fundamental parameters involved in the vibrational behaviour of the beam. Such parameters depend on both the material properties and the beam geometry. Some new characteristic maps related to the eigenvalues nature of the studied system have been provided, that can be drawn for each natural frequency of the beam. In comparison to the existing maps presented in literature for a sdof system, these maps may help in determining the parameter compounds needed to enhance or suppress certain frequency peaks, one at a time or more simultaneously, and the same approach can be exploited for any kind of mdof system. Interestingly, it has been observed that, by maintaining constant the thickness of the beam cross section, the dimensionless beam length can be utilized as key parameter to properly adjust the resonant peaks, once the material has been selected. The presented study, hence, enables to conveniently design a viscoelastic beam, in order to obtain the most suitable dynamics in the frequency range of interest, thus becoming a powerful tool for many applications, from system damping control to materials characterization.

VIII. REFERENCES

-
- [1] Bottiglione F., Carbone G., Mangialardi L., Mantriota G., Leakage Mechanism in Flat Seals, *Journal of Applied Physics* 106 (10), 104902, (2009).

- [2] Carbone G., Pierro E., Gorb S., Origin of the superior adhesive performance of mushroom shaped microstructured surfaces, *Soft Matter* 7 (12), 5545-5552, DOI:10.1039/C0SM01482F, (2011).
- [3] Carbone G., Pierro E., Sticky bio-inspired micropillars: Finding the best shape, *SMALL*, 8 (9), 1449-1454, (2012).
- [4] Carbone G., Pierro E., Effect of interfacial air entrapment on the adhesion of bio-inspired mushroom-shaped micro-pillars, *Soft Matter*, 8 (30), 7904-7908, (2012).
- [5] Carbone G., Pierro E., A review of adhesion mechanisms of mushroom-shaped microstructured adhesives, *Meccanica*, 48(8), 1819-1833, (2013).
- [6] Persson B.N.J., Rolling friction for hard cylinder and sphere on viscoelastic solid, *Eur. Phys. J. E* 33, 327-333 (2010).
- [7] Dumitru N. Olaru, Ciprian Stamate, Gheorghe Prisacaru, Rolling Friction in a Micro Tribosystem, *Tribol Lett* , 35:205–210, (2009).
- [8] G. Carbone, C. Putignano, A novel methodology to predict sliding and rolling friction of viscoelastic materials: Theory and experiments, *Journal of the Mechanics and Physics of Solids*, Volume 61, Issue 8, pp. 1822-1834, (2013).
- [9] Grosch K. A. , The Relation between the Friction and Visco-Elastic Properties of Rubber, *Proceedings of the Royal Society of London. Series A, Mathematical and Physical*, 274-1356, pp. 21-39, (1963).
- [10] Carbone G., Mangialardi L., Adhesion and friction of an elastic half-space in contact with a slightly wavy rigid surface, *Journal of the Mechanics and Physics of Solids*, 52 (6), 1267-1287, 2004.
- [11] Carbone G., Lorenz B., Persson B.N.J. and Wohlers A., Contact mechanics and rubber friction for randomly rough surfaces with anisotropic statistical properties, *The European Physical Journal E – Soft Matter*, 29 (3), 275–284, (2009)
- [12] Persson B.N.J., Theory of rubber friction and contact mechanics, *Journal of Chemical Physics*, 115, 3840 -3861 (2001).
- [13] Carbone G., Persson B.N.J., Hot cracks in rubber: origin of the giant toughness of rubber-like materials, *Physical Review Letters*, 95, 114301 (2005).
- [14] Carbone G., Persson B.N.J.: “Crack motion in viscoelastic solids: The role of the flash temperature”, *the European Physical Journal E-Soft Matter* 17 (3), 261 (2005).

- [15] Persson BNJ; Albohr O; Heinrich G; et al., Crack propagation in rubber-like materials, JOURNAL OF PHYSICS-CONDENSED MATTER 17 (44), R1071-R1142, doi: 10.1088/0953-8984/17/44/R01, (2005)
- [16] Carbone G., Persson B.N.J., Dewetting at Soft Viscoelastic Interfaces, The Journal of Chemical Physics, 121 (5): 2246-2252 (2004).
- [17] Rasa A., Applying dynamic mechanical analysis to research and development for viscoelastic damping materials, Internoise 2014 - Melbourne, Australia - Novembre 16-19, 2014.
- [18] Caracciolo R., Gasparetto A., Giovagnoni M., Measurement of the isotropic dynamic Young's modulus in a seismically excited cantilever beam using a laser sensor, Journal of Sound and Vibration 231(5), 1339-1353, (2000).
- [19] Caracciolo R., Gasparetto A., Giovagnoni M., An experimental technique for complete dynamic characterization of a viscoelastic material, Journal of Sound and Vibration 272, 1013–1032, (2004).
- [20] Cortes F. , Elejabarrieta M.J., Viscoelastic materials characterisation using the seismic response, Materials and Design, 28, 2054–2062, (2007).
- [21] Muller P., Are the eigensolutions of a 1-d.o.f. system with viscoelastic damping oscillatory or not?, Journal of Sound and Vibration 285, 501–509, (2005).
- [22] García-Barruetaña J., Cortés F., Abete J. M., Influence of Nonviscous Modes on Transient Response of Lumped Parameter Systems With Exponential Damping, Journal of Vibration and Acoustics, 133, (2011).
- [23] Adhikari S., Dynamics of Nonviscously Damped Linear Systems, J. Eng. Mech., 128:328-339, (2002).
- [24] Lázaro M., Pérez-Aparicio L., Epstein M., A viscous approach based on oscillatory eigensolutions for viscoelastically damped vibrating systems, Mechanical Systems and Signal Processing, 40, 767–782, (2013).
- [25] García-Barruetaña J., Cortés F., Abete J. M., Dynamics of an exponentially damped solid rod: Analytic solution and finite element formulations, International Journal of Solids and Structures 49, 590–598, (2012).
- [26] Inman D. J., Vibration analysis of viscoelastic beams by separation of variables and modal analysis, Mechanics Research Communications, Vol.16(4), 213-218, (1989).
- [27] Gupta A.K., Khanna A., Vibration of visco-elastic rectangular plate with linearly thickness

- variations in both directions, *Journal of Sound and Vibration* 30, 450–457, (2007).
- [28] Adhikari S., Qualitative dynamic characteristics of a non-viscously damped oscillator, *Proc. R. Soc. A*, 461, 2269–2288, (2005).
 - [29] Christensen R. M., *Theory of viscoelasticity*, Academic Press, New York.
 - [30] Inman D. J., *Engineering Vibrations*, Prentice Hall, isbn: 0-13-518531-9, (1996).
 - [31] H. T. Banks and D. J. Inman , On Damping Mechanisms in Beams, *J. Appl. Mech* 58(3), 716-723, (1991).
 - [32] Thomson WT, Dahleh MD, "Theory of vibration with applications", 5th edn. Prentice Hall, Englewood Cliffs, (1997).
 - [33] Abramowitz, M., and Stegun, I. A., 1965, *Handbook of Mathematical Functions*, With Formulas, Graphs, and Mathematical Tables, Dover Publications, New York.
 - [34] Lazard D., "Quantifier elimination: Optimal solution for two classical examples". *Journal of Symbolic Computation*, 5: 261–266, (1988).
 - [35] Rees E. L., "Graphical Discussion of the Roots of a Quartic Equation", *The American Mathematical Monthly*, 29 (2): 51–55, (1922).
 - [36] S. W. Park, R. A. Schapery, "Methods of interconversion between linear viscoelastic material functions. Part I - a numerical method based on Prony series, *International Journal of Solids and Structures*, 36, 1653-1675, (1999).